

Preparation and crystal structure of a new bismuth chromate: $\text{Bi}_8(\text{CrO}_4)\text{O}_{11}$

N. Kumada^{a,*}, T. Takei^a, N. Kinomura^a, G. Wallez^b

^aDepartment of Research Interdisciplinary Graduate School of Medicine and Engineering, University of Yamanashi, Miyamae-cho 7, Kofu 400-8511 Japan

^bLaboratoire de Chimie et Propriétés de la Matière Condensée de Paris, Université Pierre et Marie Curie, 4 place Jussieu, 75252 Paris Cedex 05, France

Received 20 October 2005; received in revised form 22 November 2005; accepted 22 November 2005

Available online 20 January 2006

Abstract

Single crystals of a new bismuth chromate, $\text{Bi}_8(\text{CrO}_4)\text{O}_{11}$, were prepared by hydrothermal reaction of $\text{NaBiO}_3 \cdot n\text{H}_2\text{O}$ in K_2CrO_4 solution. The bismuth chromate crystallizes in the monoclinic space group $P2_1/m$ with $a = 9.657(3)$, $b = 11.934(3)$, $c = 13.868(2)\text{Å}$ and $\beta = 104.14(1)^\circ$, $Z = 4$ and the final R factors are $R = 0.038$ and $R_w = 0.041$ for 3541 unique reflections. The crystal structure has a slab built up by $(\text{CrO}_4)^{2-}$ tetrahedra and distorted bismuth polyhedra which are five-fold pyramids, six-fold trigonal prisms and octahedra. The distance of lone pair from nucleus for bismuth atoms ranges from 0.29 to 1.12 Å, depending on the coordination environment. $\text{Bi}_8(\text{CrO}_4)\text{O}_{11}$ decomposes to $\text{Bi}_{14}\text{CrO}_{24}$ and a small amount of an unknown phase at 796 °C.

© 2005 Elsevier Inc. All rights reserved.

Keywords: Bismuth oxide; Hydrothermal reaction; Crystal structure; Lone pair

1. Introduction

We have prepared a variety of new bismuth oxides by low-temperature hydrothermal reactions using hydrate sodium bismuth oxide, $\text{NaBiO}_3 \cdot n\text{H}_2\text{O}$ [1–8]. One of them, $\text{HBi}_3(\text{CrO}_4)_2\text{O}_3$ was prepared by using $\text{Cr}(\text{NO}_3)_3$ solution and its crystal structure was determined by using single crystal X-ray diffraction data [3]. So far several bismuth chromium oxides and oxyhydroxides have been reported, for example, $\text{Bi}_2(\text{CrO}_4)_2\text{Cr}_2\text{O}_7$ [9], BiOHCrO_4 [10], perovskite-type BiCrO_3 prepared under high pressure [11] and the orthorhombic phase BiCrO_3 prepared by an usual calcination method [12]. Recently, a new bismuth chromate, $\text{Bi}_6\text{Cr}_2\text{O}_{15}$, was reported [13], having the unique $(\text{Bi}_{12}\text{O}_{14})^{8n+n}$ columns as found in $\text{Bi}_{13}\text{Mo}_4\text{VO}_{34}$ [14]. In the bismuth rich phases in the Bi_2O_3 – Cr_2O_3 system there are two compounds; one is the cubic sillenite-type compound [15] which has the crystal structure of γ - Bi_2O_3 ,

one of the four modifications of bismuth sesquioxide, and another is $\text{Bi}_{14}\text{CrO}_{24}$ which crystal structure was determined by single crystal X-ray diffraction analysis [16]. Except for the perovskite-type BiCrO_3 , the crystal structure of bismuth chromates is built up by CrO_4 tetrahedron and Bi^{3+} with irregular coordination environment caused by stereo active lone pair.

A new bismuth chromate, $\text{Bi}_8(\text{CrO}_4)\text{O}_{11}$ was found on the course of investigation of hydrothermal reactions using $\text{NaBiO}_3 \cdot n\text{H}_2\text{O}$ and the crystal structure was determined by using single crystal X-ray diffraction data. The crystal structure and thermal behavior of this new compound will be described.

2. Experimental

2.1. Sample preparation and characterization

Reddish yellow needle-like single crystals were prepared by hydrothermal reaction. $\text{NaBiO}_3 \cdot n\text{H}_2\text{O}$ (Nacalai Tesque Inc.) was placed in a Teflon-lined autoclave (70 mL) with K_2CrO_4 ($\text{Bi}:\text{Cr} = 1:2\sim 4$) and H_2O (30 mL)

*Corresponding author. Fax: +81 55 254 3035.

E-mail address: kumada@yamanashi.ac.jp (N. Kumada).

at 180 °C for 4 days. The solid products were separated by centrifuging, washed with distilled water, and dried at 50 °C. The products were identified by X-ray powder diffraction using Ni-filtered CuK α radiation. The thermal stability was investigated by TG-DTA with a heating rate of 10 °C/min from room temperature to 1000 °C.

2.2. Structure determination

Single crystal X-ray diffraction data were collected by using a Rigaku AFC-7R four-circle diffractometer with graphite monochromated MoK α radiation using the ω – 2θ scan technique ($D\omega = (1.42 + 0.30 \tan\theta)^\circ$). The data were corrected for Lorentz and polarization effects. Absorption effects were corrected by using ψ scans. The crystal structure was solved and refined with the computer programs from the TEXSAN crystallographic software package [17]. Details of the data collection and refinement are summarized in Table 1. The final positional and anisotropic thermal parameters are summarized in Table 2. Selected interatomic distances and angles are listed in Table 3. The positions of lone pairs of bismuth atoms were determined by using the laboratory-made program HYBRIDE [18], based upon the research of the equilibrium position of the lone pair in the electrostatic field. A description of the principle of this program can be found in [19].

Table 1
Crystal data and intensity collection for Bi₈(CrO₄)O₁₁

Color	Reddish yellow
Size (mm)	0.02 × 0.02 × 0.10
Crystal system	Monoclinic
Space group	<i>P</i> 2 ₁ / <i>m</i> (No. 11), <i>Z</i> = 4
Lattice parameters	<i>a</i> = 9.657(3) Å <i>b</i> = 11.934(3) Å <i>c</i> = 13.868(2) Å β = 104.14(1)°
Volume	1549.9(6) Å ³
Formula weight	289.87
Calculated density (g/cm ³)	8.42
Diffractometer	Rigaku AFC-7R
Radiation	Graphite monochromated MoK α (λ = 0.71069 Å)
Temperature (°C)	23
μ (MoK α) (cm ^{−1})	929.10
Maximum 2θ (deg)	90
Scan mode	ω – 2θ
Scan speed (°/min)	16
Number of data collected	13554
Number of unique data	3541
Absorption correction	ψ scans
Transmission factors	0.78–0.99
Refinement method	Full-matrix least-squares on F
Number of parameters	242
<i>R</i>	0.038
<i>R</i> _w	0.041
Goodness of fit	1.18

Table 2

Atom	Site	<i>x</i>	<i>y</i>	<i>z</i>	<i>B</i> _{eq} [*] (Å ²)
<i>Positional and thermal parameters for Bi₈(CrO₄)O₁₁</i>					
Bi(1)	2e	0.6566(1)	1/4	0.73494(9)	0.88(2)
Bi(2)	2e	0.9903(1)	1/4	0.64552(9)	1.00(2)
Bi(3)	2e	0.0362(1)	1/4	0.12567(9)	1.10(3)
Bi(4)	2e	0.3378(1)	1/4	0.0236(1)	1.15(3)
Bi(5)	4f	0.3117(1)	0.09909(8)	0.76003(7)	1.22(2)
Bi(6)	4f	0.66185(1)	0.08937(8)	0.48210(6)	0.79(2)
Bi(7)	4f	0.04885(9)	0.43951(7)	0.39018(6)	0.88(2)
Bi(8)	4f	0.67037(9)	0.42796(8)	0.98818(6)	0.87(2)
Bi(9)	4f	0.34316(1)	0.42625(8)	0.24588(6)	0.93(2)
Bi(10)	4f	0.9811(1)	0.07838(8)	0.87586(7)	1.50(2)
Cr(1)	2e	0.7292(6)	1/4	0.2458(4)	1.1(1)
Cr(2)	2e	0.3576(2)	1/4	0.5182(4)	1.0(1)
O(1)	2e	0.471(3)	1/4	0.812(2)	3.2(7)
O(2)	2e	0.896(2)	1/4	0.766(2)	0.9(5)
O(3)	2e	0.194(2)	1/4	0.758(2)	1.5(5)
O(4)	2e	0.189(3)	1/4	0.528(2)	2.4(6)
O(5)	2e	0.360(3)	1/4	0.401(2)	1.9(6)
O(6)	2e	0.902(3)	1/4	0.285(2)	2.4(6)
O(7)	2e	0.700(3)	1/4	0.129(2)	2.7(7)
O(8)	2e	0.288(2)	1/4	0.178(2)	1.3(5)
O(9)	2e	0.110(2)	1/4	0.991(1)	0.6(4)
O(10)	2e	0.732(3)	1/4	0.534(2)	1.7(5)
O(11)	4f	0.334(2)	0.866(2)	0.719(2)	3.8(6)
O(12)	4f	0.285(2)	0.067(2)	0.900(1)	1.6(4)
O(13)	4f	0.893(2)	0.428(1)	0.014(1)	0.9(3)
O(14)	4f	0.717(2)	0.107(1)	0.831(1)	1.2(3)
O(15)	4f	0.065(1)	0.068(1)	0.701(1)	0.8(3)
O(16)	4f	0.745(1)	0.026(1)	0.625(1)	0.8(3)
O(17)	4f	0.877(1)	0.047(1)	0.480(1)	0.8(3)
O(18)	4f	0.437(2)	0.139(2)	0.575(1)	1.7(4)
O(19)	4f	0.119(2)	0.420(1)	0.197(1)	0.9(3)
O(20)	4f	0.387(2)	0.075(1)	0.098(1)	1.5(4)

Atom	<i>U</i> ₁₁	<i>U</i> ₂₂	<i>U</i> ₃₃	<i>U</i> ₁₂	<i>U</i> ₁₃	<i>U</i> ₂₃
<i>Anisotropic thermal parameters for Bi₈(CrO₄)O₁₁</i>						
Bi(1)	0.0139(6)	0.0077(6)	0.0091(6)	0	−0.0022(4)	0
Bi(2)	0.0132(6)	0.0151(7)	0.0084(6)	0	−0.0001(4)	0
Bi(3)	0.0165(6)	0.0152(7)	0.0103(6)	0	0.0035(5)	0
Bi(4)	0.0151(6)	0.0135(7)	0.0155(6)	0	0.0044(5)	0
Bi(5)	0.0198(4)	0.0173(5)	0.0109(4)	0.0060(4)	0.0067(3)	0.0024(3)
Bi(6)	0.0113(4)	0.0100(4)	0.0077(4)	−0.0005(3)	0.0007(3)	0.0009(3)
Bi(7)	0.0154(4)	0.0070(5)	0.0095(4)	−0.0002(3)	0.0001(3)	−0.0003(3)
Bi(8)	0.0115(4)	0.0092(4)	0.0116(4)	−0.0009(3)	0.0015(3)	0.0019(3)
Bi(9)	0.0121(4)	0.0142(5)	0.0078(4)	−0.0011(3)	−0.0002(3)	0.0002(3)
Bi(10)	0.0265(5)	0.0139(5)	0.0176(5)	−0.0051(4)	0.0069(3)	−0.0033(4)
Cr(1)	0.023(3)	0.008(3)	0.006(3)	0	−0.003(2)	0
Cr(2)	0.012(3)	0.013(3)	0.009(3)	0	−0.003(2)	0
O(1)	0.02(2)	0.07(2)	0.02(2)	0	−0.01(1)	0
O(2)	0.01(1)	0.02(1)	0.01(1)	0	0.009(8)	0
O(3)	0.00(1)	0.02(1)	0.03(1)	0	−0.014(9)	0
O(4)	0.02(2)	0.04(2)	0.02(2)	0	0.00(1)	0
O(5)	0.04(1)	0.03(2)	0.01(1)	0	0.02(1)	0
O(6)	0.04(2)	0.02(2)	0.03(2)	0	0.00(1)	0
O(7)	0.06(2)	0.02(2)	0.02(2)	0	0.01(1)	0
O(8)	0.02(1)	0.01(1)	0.02(1)	0	0.001(9)	0
O(9)	0.00(1)	0.02(1)	0.00(1)	0	−0.006(8)	0
O(10)	0.02(1)	0.02(1)	0.02(1)	0	0.00(1)	0
O(11)	0.05(1)	0.04(2)	0.05(1)	−0.03(1)	0.01(1)	0.01(1)
O(12)	0.038(9)	0.02(1)	0.009(9)	0.010(8)	0.012(7)	0.006(8)
O(13)	0.004(8)	0.015(9)	0.018(8)	−0.003(6)	0.008(6)	−0.008(7)
O(14)	0.019(8)	0.013(9)	0.011(8)	0.006(6)	0.000(6)	0.003(7)
O(15)	0.007(7)	0.006(8)	0.015(7)	0.004(6)	0.002(5)	−0.007(6)
O(16)	0.014(7)	0.017(9)	0.002(8)	−0.005(6)	0.003(6)	−0.001(6)
O(17)	0.013(7)	0.009(8)	0.004(8)	0.006(6)	−0.005(5)	0.006(6)
O(18)	0.025(9)	0.01(1)	0.028(9)	0.008(8)	0.001(7)	−0.010(8)
O(19)	0.007(7)	0.003(8)	0.020(7)	0.007(6)	−0.002(5)	0.008(7)
O(20)	0.029(9)	0.02(1)	0.010(9)	−0.003(7)	0.001(6)	0.000(8)

$$B_{\text{eq}}^* = (8\pi^2/3)\sum_i \Sigma_j U_{ij} a_i^* a_j^* a_i a_j$$

Table 3
Selected interatomic distances (Å) for $\text{Bi}_8(\text{CrO}_4)\text{O}_{11}$

Cr(1)–O(6)	1.63(3)	Cr(2)–O(4)	1.66(3)
Cr(1)–O(7)	1.58(3)	Cr(2)–O(5)	1.63(3)
Cr(1)–O(11)	1.63(3) × 2	Cr(2)–O(18)	1.64(2) × 2
Mean	1.62	Mean	1.64
Bi(1)–O(1)	2.30(3)	Bi(2)–O(2)	2.09(2)
Bi(1)–O(2)	2.24(2)	Bi(2)–O(3)	2.19(2)
Bi(1)–O(14)	2.16(2) × 2	Bi(2)–O(4)	2.80(3)
Bi(1)–O(18)	2.98(2) × 2	Bi(2)–O(10)	2.59(2)
Mean	2.47	Bi(2)–O(15)	2.36(2) × 2
		Mean	2.40
Bi(3)–O(6)	2.82(3)	Bi(4)–O(8)	2.30(2)
Bi(3)–O(8)	2.37(2)	Bi(4)–O(9)	2.13(2)
Bi(3)–O(9)	2.16(2)	Bi(4)–O(12)	2.75(2) × 2
Bi(3)–O(13)	2.79(2) × 2	Bi(4)–O(20)	2.33(2) × 2
Bi(3)–O(19)	2.31(2) × 2	Mean	2.43
Mean	2.51		
Bi(5)–O(1)	2.36(2)	Bi(6)–O(10)	2.102(9)
Bi(5)–O(3)	2.13(1)	Bi(6)–O(11)	2.85(2)
Bi(5)–O(11)	2.86(3)	Bi(6)–O(16)	2.08(1)
Bi(5)–O(12)	2.06(2)	Bi(6)–O(17)	2.15(1)
Bi(5)–O(15)	2.36(1)	Bi(6)–O(18)	2.85(2)
Mean	2.35	Bi(6)–O(18)	2.93(2)
		Mean	2.49
Bi(7)–O(6)	2.87(2)	Bi(8)–O(7)	2.85(2)
Bi(7)–O(15)	2.11(1)	Bi(8)–O(12)	2.24(2)
Bi(7)–O(16)	2.30(1)	Bi(8)–O(13)	2.09(1)
Bi(7)–O(17)	2.19(1)	Bi(8)–O(14)	2.37(2)
Bi(7)–O(17)	2.31(1)	Bi(8)–O(20)	2.12(2)
Bi(7)–O(19)	2.93(2)	Mean	2.33
Mean	2.45		
Bi(9)–O(5)	2.99(2)	Bi(10)–O(2)	2.57(1)
Bi(9)–O(8)	2.313(9)	Bi(10)–O(9)	2.70(1)
Bi(9)–O(14)	2.42(2)	Bi(10)–O(12)	2.87(2)
Bi(9)–O(16)	2.47(2)	Bi(10)–O(13)	2.28(2)
Bi(9)–O(19)	2.10(1)	Bi(10)–O(13)	2.47(2)
Bi(9)–O(20)	2.19(2)	Bi(10)–O(14)	2.49(2)
Mean	2.41	Bi(10)–O(15)	2.74(1)
		Bi(10)–O(19)	2.25(2)
		Mean	2.55

3. Results and discussion

3.1. Crystal structure

The crystal structure of $\text{Bi}_8(\text{CrO}_4)\text{O}_{11}$ has a slab built up by $(\text{CrO}_4)^{2-}$ tetrahedra and Bi^{3+} coordinated by 5–8 oxygen atoms, and the slabs are stacked along the *a*-axis as shown in Fig. 1. In this figure the Bi–O bondings with the length of $d < 3.0 \text{ \AA}$ and the location of lone pairs are represented. The distances of the lone pairs from the nuclei are listed in Table 4. The slab of $\text{Bi}_8(\text{CrO}_4)\text{O}_{11}$ is composed of three metal layers in which the Bi layer (layer I) is sandwiched by the Cr, Bi layers (layer II). The feature of this crystal structure is similar to that of $\text{HBi}_3(\text{CrO}_4)_2\text{O}_3$ [3] which has two types of slabs; one is composed of one Bi layer and two

Table 4
Distances (Å) of lone pair from nucleus for bismuth atom

Layer I		Layer II	
Bi(2)	0.87	Bi(1)	0.69
Bi(3)	0.53	Bi(4)	0.50
Bi(7)	0.58	Bi(5)	1.12
Bi(10)	0.39	Bi(6)	0.54
		Bi(8)	0.82
		Bi(9)	0.29

Cr, Bi layers like that of $\text{Bi}_8(\text{CrO}_4)\text{O}_{11}$ and another is two Cr, Bi layers as shown in Fig. 2.

The various coordination environments of Bi atoms in this compound cannot be understood at first glance from Fig. 1. For easier viewing the layers I and II are separately drawn in Fig. 3 and their polyhedral representation is shown in Fig. 4. The layer I has four distinct Bi sites (Bi(2), Bi(3), Bi(7) and Bi(10)), and two types of chains connected by edge-sharing run along the *b*-axis; one is connected by edge-sharing Bi(3)O_7 and Bi(10)O_8 and another is by corner-sharing Bi(2)O_6 and Bi(7)O_6 octahedra. On the other hand the layer II has four types of chains connected by corner- and edge-sharing along the *b*-axis. Every chain is formed by edge- and/or corner-sharing polyhedra as observed in the layer I. The combinations are Bi(6)O_6 octahedra and Cr(2)O_4 tetrahedra, Bi(5)O_5 square pyramids and Cr(1)O_4 tetrahedra, Bi(4)O_6 trigonal prisms and Bi(8)O_5 pyramids, and Bi(1)O_6 and Bi(9)O_6 octahedra. Although all Bi polyhedra are strongly deformed from a regular shape, the two types of CrO_4 tetrahedra are almost regular ones. The mean Cr–O distances in the tetrahedra are 1.62 and 1.64 Å for Cr(1) and Cr(2), respectively, and these values agree with those (1.66–1.67 Å) for $\text{HBi}_3(\text{CrO}_4)_2\text{O}_3$ [3] and $\text{Bi}_{14}\text{CrO}_{24}$ [14].

There are four short Bi–Bi contacts in this compound. One is observed between edge-sharing Bi(5)O_5 pyramids as found in $\text{Ca}_4\text{Bi}_6\text{O}_{13}$ [20] and the corresponding Bi–Bi distances are similar to each other (3.601 Å for this compound and 3.604 Å for $\text{Ca}_4\text{Bi}_6\text{O}_{13}$). The differences between edge-sharing BiO_5 pyramids of the two compounds are the shape and configuration of the pyramids. In $\text{Ca}_4\text{Bi}_6\text{O}_{13}$ the basal faces of two BiO_5 pyramids are almost square and are edge-sharing in the way that the basal faces are coplanar, while in this compound, Bi(5)O_5 pyramids are strongly deformed and the basal faces are not coplanar. The other short Bi–Bi contacts are observed between the layers I and II; the distances of Bi(6)–Bi(7), Bi(3)–Bi(4) and Bi(2)–Bi(5) are 3.424, 3.536 and 3.603 Å, respectively. For every short Bi–Bi contact the corresponding polyhedra are edge-sharing and the other edge-sharings in this compound have long Bi–Bi distance with $\geq 3.66 \text{ \AA}$ for Bi(8)–Bi(9) or Bi(9)–Bi(10).

Strong deformation of Bi polyhedra which comes from a stereo active lone pair of Bi^{3+} is found in a lot

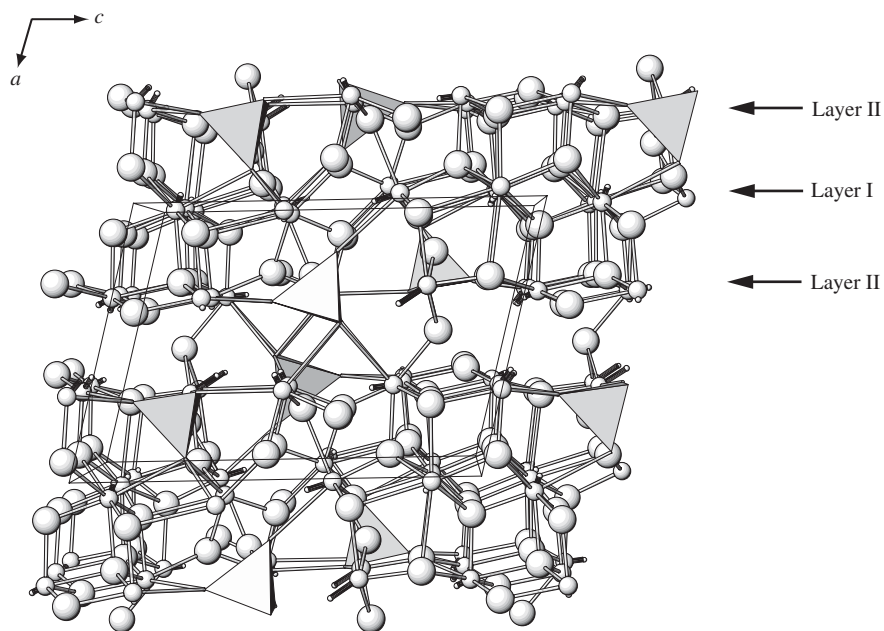


Fig. 1. Crystal structure of $\text{Bi}_8(\text{CrO}_4)\text{O}_{11}$.

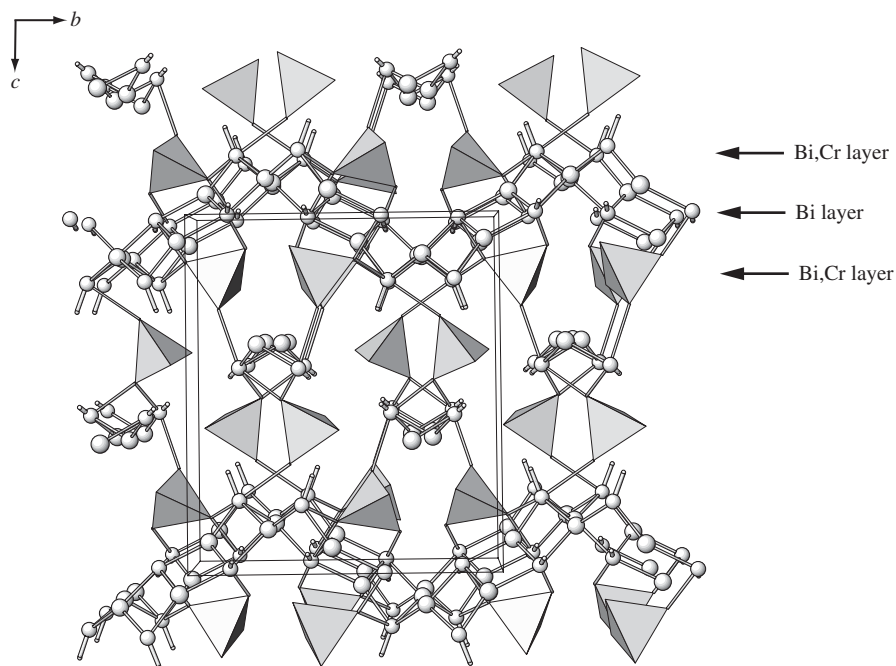


Fig. 2. Crystal structure of $\text{HBi}_3(\text{CrO}_4)_2\text{O}_3$.

of Bi^{3+} oxides. The mean Bi–O distances (2.35–2.55 Å) in this compound correspond to those for the other bismuth chromates; (2.56–2.59 Å) for $\text{HBi}_3(\text{CrO}_4)_2\text{O}_3$ (3), (2.237–2.432 Å) for $\text{Bi}_6\text{Cr}_2\text{O}_{15}$ (13) and (2.54–2.72 Å) for $\text{Bi}_{14}\text{CrO}_{24}$ [14]. Fig. 5 shows the plot of the distance of lone pair from the nucleus against mean Bi–O distance for Bi^{3+}

in 22 complex bismuth oxides from which mixed valence compounds and perovskite-type compounds having Bi^{3+} in the A site are excluded. Most of Bi^{3+} oxides have the mean Bi–O distance of 2.3–2.5 Å and the distance of lone pair from the nucleus is inclined to decrease with increase of the mean Bi–O distance. This tendency can be explained

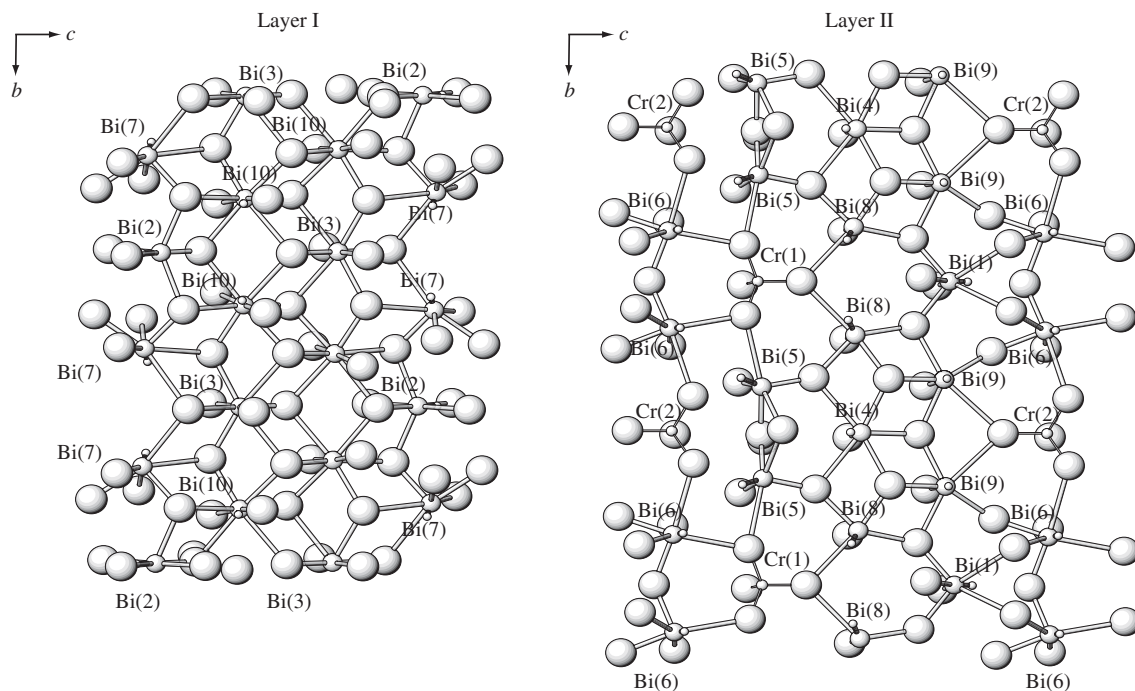


Fig. 3. Layers I and II in $\text{Bi}_8(\text{CrO}_4)\text{O}_{11}$.

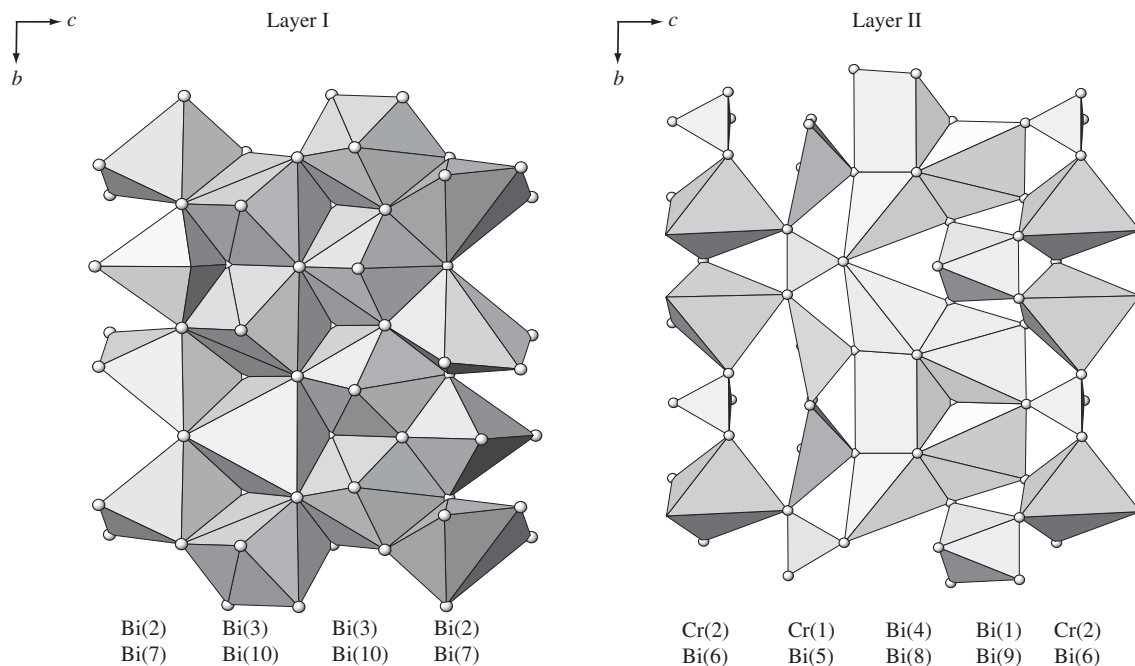


Fig. 4. Polyhedral representation of $\text{Bi}_8(\text{CrO}_4)\text{O}_{11}$.

qualitatively by the coordination environment of Bi^{3+} . Generally mean Bi–O distance depends on the coordination number (CN); the Bi atom with longer mean Bi–O distance has bigger CN and smaller CN makes mean Bi–O distance shorter. Since the Bi atom with bigger CN does not have the room enough to accommodate the lone pair,

the lone pair must be brought close to the nucleus. On the contrary the Bi atom with smaller CN can put the lone pair far from the nucleus. The shortest Bi–O distances ($\sim 2 \text{ \AA}$) are in the range of classical Bi^{5+} –O bonds, accounting for a strong stereochemical effect of the lone pair that points toward the opposite direction. Actually, Bi^{3+} with the

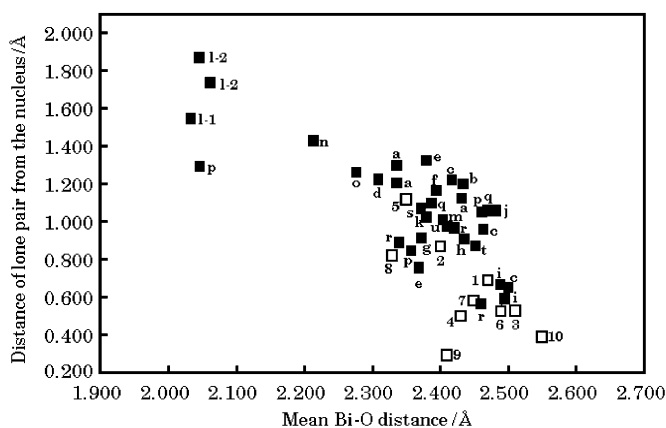


Fig. 5. Distance of lone pair from the nucleus vs. mean Bi–O distance for various bismuth oxides. One to two correspond to Bi(1)–Bi(10) in this compound: a; $\text{Bi}_6\text{Cr}_2\text{O}_{15}$ [13], b; $\text{Bi}_2\text{Al}_4\text{O}_9$ [24], c; $\text{HBi}_3(\text{CrO}_4)_2\text{O}_3$ [3], d; $\text{Bi}_{4.86}\text{La}_{1.14}\text{O}_9$ [23], e; $\text{Bi}_2\text{W}_2\text{O}_9$ [25], f; $\alpha\text{-BiNbO}_4$ [26], g; $\text{SrBi}_2\text{Nb}_2\text{O}_9$ [27], h; $\text{BaBi}_2\text{Nb}_2\text{O}_9$ [27], i; $\text{Bi}_2\text{Mo}_3\text{O}_{12}$ [28], j; $\alpha\text{-Bi}_2\text{Ti}_4\text{O}_{11}$ [29], k; $\beta\text{-Bi}_2\text{Ti}_4\text{O}_{11}$ [29], l-1; $\text{Sr}_2\text{Bi}_2\text{O}_5$ [21], l-2; $\text{Sr}_2\text{Bi}_2\text{O}_5$ [22], m; Bi_2CuO_4 [30], n; NaBiO_2 [31], o; KBiO_2 [32], p; $\text{Ca}_4\text{Bi}_6\text{O}_{13}$ [20], q; Bi_2MoO_6 [33], r; Bi_3SbO_7 [34], s; Bi_2WO_6 [35], t; $\text{K}_{0.5}\text{Bi}_{2.5}\text{Nb}_2\text{O}_9$ [36], u; $\text{Na}_{0.5}\text{Bi}_{2.5}\text{Nb}_2\text{O}_9$ [36].

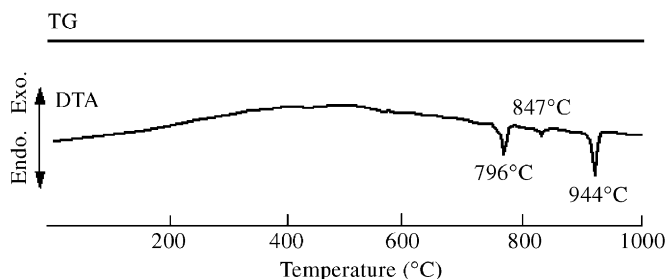


Fig. 6. TG-DTA curves of $\text{Bi}_8(\text{CrO}_4)\text{O}_{11}$.

short Bi–O distance of $\sim 2 \text{ \AA}$ in $\text{Ca}_4\text{Bi}_6\text{O}_{13}$ [19] and $\text{Sr}_2\text{Bi}_2\text{O}_5$ [21,22] (CN = 3) have a long distance of lone pair from the nucleus (1.3–1.8 Å), while Bi(9) (Bi–O; 2.41 Å) with CN = 6 and Bi(10) (Bi–O; 2.55 Å) with CN = 8 in this compound have a short distance to the lone pair (0.29 and 0.39 Å, respectively).

3.2. Thermal behavior

The TG-DTA curves of $\text{Bi}_8(\text{CrO}_4)\text{O}_{11}$ are shown in Fig. 6. No weight loss was observed in the TG curve and three endothermic peaks were observed at 796, 847 and 944 °C in the DTA curve. The strongest peak at 944 °C corresponds to the melt of the sample and the one at 796 °C to decomposition to $\text{Bi}_{14}\text{CrO}_{24}$ and a small amount of an unknown phase, which was confirmed by X-ray powder diffraction pattern. The weakest one appears at 847 °C, but no change after cooling in the X-ray powder diffraction patterns taken above and below the temperature was observed. The corresponding peak was not observed during the cooling. This weak endothermic peak may be related to the unknown phase.

Acknowledgments

This work was supported by Grant-in-Aid for Scientific Research (C) (12650668) from the Ministry of Education, Science and Culture, Japan.

References

- [1] N. Kumada, M. Hosoda, N. Kinomura, *J. Solid State Chem.* 106 (1993) 476–484.
- [2] N. Kumada, N. Kinomura, S. Kodialam, A.W. Sleight, *Mater. Res. Bull.* 29 (1994) 497–503.
- [3] S. Kodialam, N. Kumada, R. Mackey, A.W. Sleight, *Eur. J. Solid State Inorg. Chem.* 31 (1994) 739–746.
- [4] N. Kinomura, N. Kumada, *Mater. Res. Bull.* 30 (1995) 129–134.
- [5] N. Kumada, N. Kinomura, P.M. Woodward, A.W. Sleight, *J. Solid State Chem.* 116 (1995) 281–285.
- [6] N. Kumada, N. Kinomura, N. Takahashi, A.W. Sleight, *J. Solid State Chem.* 126 (1996) 121–126.
- [7] N. Kumada, N. Kinomura, N. Takahashi, A.W. Sleight, *Mater. Res. Bull.* 32 (1997) 1003–1008.
- [8] N. Kumada, N. Kinomura, in: S.M. Kauzlarich, E.M. MacCarron III, A.W. Sleight, H.-C. zur Loye (Eds.), *Solid State Chemistry Inorganic Materials II*, vol. 547, *Mater. Res. Soc. Proc.*, Boston, MA, 1998, p. 227.
- [9] Y. Gerault, A. Riou, Y. Cudennec, A. Bonnin, *Revue Chimie Minerale* 24 (1987) 631–640.
- [10] B. Aurivillius, A. Lowenhielm, *Acta Chem. Scand.* 18 (1964) 1937–1957.
- [11] F. Sugawara, S. Iida, Y. Syono, S. Akimoto, *J. Phys. Soc. Japan* 20 (1965) 1529.
- [12] K. Masuno, *J. Chem. Soc. Japan* 90 (1969) 1122–1127.
- [13] J. Grins, S. Esmailzadeh, S. Hull, *J. Solid State Chem.* 163 (2002) 144–150.
- [14] R. Enjalbert, G. Hasselmann, J. Galy, *J. Solid State Chem.* 131 (1997) 236–245.
- [15] I.D. Zhitomirskii, S.V. Fedotov, N.E. Skorokhodov, A.A. Bush, A. Mari'n, Yu.N. Venetsev, *Russ. J. Inorg. Chem.* 28 (1983) 570–573.
- [16] S.A. Warda, W. Pietzuch, W. Massa, U. Kesper, D. Reinen, *J. Solid State Chem.* 149 (2000) 209–217.
- [17] Molecular Structure Corporation, TEXSAN, The Woodlands, TX, 1993.
- [18] G. Wallez, *HYBRIDE: A Program for the Research of Lone Pairs Positions in Crystalline Solids*, Universite Pierre et Marie Curie, France, 1999.
- [19] E. Morin, G. Wallez, S. Jaulmes, J.C. Couturier, M. Quarton, *J. Solid State Chem.* 137 (1998) 283–288.
- [20] J.B. Parise, C.C. Torardi, M.H. Whangbo, C.J. Rawn, R.S. Roth, B.P. Burto, *Chem. Mater.* 2 (1990) 454–458.
- [21] J.F. Vente, R.B. Helmholtz, D.J.W. Ijdo, *Acta Crystallogr. C* 48 (1992) 1380–1382.
- [22] C.C. Torardi, J.B. Parise, A. Santoro, C.J. Rawn, R.S. Roth, B.P. Burton, *J. Solid State Chem.* 93 (1991) 228–235.
- [23] S. Obbade, M. Drache, P. Conflant, E. Suard, *J. Solid State Chem.* 162 (2001) 10–19.
- [24] I. Abrahams, A.J. Bush, G.E. Hawkes, T. Nunes, *J. Solid State Chem.* 147 (1999) 631–636.
- [25] J.C. Champarnaud-Mesjard, B. Frit, A. Watanabe, *J. Mater. Chem.* 9 (1999) 1319–1322.
- [26] M.A. Subramanian, J.C. Calabrese, *Mater. Res. Bull.* 28 (1993) 523–529.
- [27] Ismunandar, B.J. Kennedy, Gunawan, Marsongkohadi, *J. Solid State Chem.* 126 (1996) 135–141.
- [28] A.F. van den Elzen, G.D. Rieck, *Acta Crystallogr. B* 29 (1973) 2433–2436.
- [29] W. Kahenberg, H. Boehm, *Acta Crystallogr. B* 51 (1995) 11–18.

- [30] M.T. Weller, D.R. Lines, *J. Solid State Chem.* 82 (1989) 21–29.
- [31] B. Schwedes, R. Hoppe, *Z. Anorg. Allg. Chem.* 391 (1972) 313–322.
- [32] B. Schwedes, R. Hoppe, *Z. Anorg. Allg. Chem.* 392 (1972) 97–106.
- [33] R.G. Teller, J.F. Brazdil, R.K. Grasselli, J.D. Jorgensen, *Acta Crystallogr. C* 40 (1984) 2001–2005.
- [34] R.E. Dinnebier, R.M. Ibberson, H. Ehrenberg, M. Jansen, *J. Solid State Chem.* 163 (2002) 332–339.
- [35] K.S. Knight, *Miner. Mag.* 56 (1992) 399–409.
- [36] S. Borg, G. Svensson, *J. Solid State Chem.* 156 (2001) 160–165.